Available online at www.sciencedirect.com
SCIENCE DIRECT®
Journal of Molecular Catalysis A: Chemical 229 (2005) 77–85
JOURNAL OF MOLECULAR CATALYSIS A: CHEMICAL
www.elsevier.com/locate/molcata

An ab initio study of ethane conversion reactions on zeolites using the complete basis set composite energy method

Xiaobo Zheng, Paul Blowers*

Department of Chemical and Environmental Engineering, The University of Arizona, PO Box 210011, Tucson, AZ 85721 0011, USA

Received 24 September 2004; received in revised form 5 November 2004; accepted 6 November 2004
Available online 22 December 2004

Abstract

Ab initio methods are used to study the transition state structures and activation energies of ethane cracking, hydrogen exchange, and dehydrogenation reactions catalyzed by a zeolite model cluster. The reactant and transition state structures are optimized by HF and MP2 methods and the final energies are calculated using a complete basis set composite energy method. The computed activation barriers are 71.39 kcal/mol for cracking, 31.39 kcal/mol for hydrogen exchange and 75.95 kcal/mol for dehydrogenation using geometries optimized with the MP2 method. The effects of cluster size and acidity on the reaction barriers are also investigated. The relationships between activation barriers and zeolite deprotonation energies for each reaction are proposed so that accurate activation energies can be obtained when using different zeolites as catalysts.

Keywords: Zeolite; Ethane; Cluster approach; CBS method

1. Introduction

Zeolites are crystalline aluminosilicates with a three-dimensional framework structure which forms uniformly sized pores of molecular dimension. They are broadly used as catalysts in the oil refining and petroleum industries; the world wide total annual zeolite catalyst consumption rate was 360 million tonnes in 1998 [1]. There are hundreds of different zeolite structures, and by applying increased computing power to structure resolution, 130 types have been identified and described in the International Zeolite Association Database [2]. Of those 130 types, about 16 are of commercial interest and are produced synthetically. In order to identify different zeolite structures, a three-letter framework code is generally accepted to describe the different zeolite structures, e.g. FAU for the mineral faujasite, LTA for Linde Type A, and MFI for ZSM-5 (Zeolite SOCONY Mobile – five) [3].

A zeolite has a lattice structure. When all of the lattice ions are silicon, the zeolite lattice's composition is SiO_2, a polymorph of quartz. Brønsted acidic sites are formed when a silicon atom, which has a formal valency of 4, is replaced by an aluminum atom with a valency of 3. A proton is attached to the oxygen atom connecting the silicon and its aluminum atom neighbor, resulting in a chemically stable structure where the oxygen atom becomes a three-coordinated structure. SiO and AlO bonds have considerable covalency, resulting in a relatively weak OH bond. The 'onium' type coordination of oxygen is the fundamental reason for the high acidity of the attached proton, which makes a zeolite a good catalyst [4].

The conversion of hydrocarbons by zeolite acid catalysts is essential for the modern oil and chemical industries [5,6]. The heterogeneous catalytic reactions which occur on zeolite surfaces can be studied with computational methods using either the cluster approach or embedding methods, depending upon the character of the reactions. A cluster model is formed by cutting out a small portion of the catalyst lattice and terminating the open valences with hydroxyl or hydride bonds. The cluster size is chosen so that the reaction can be modeled using quantum methods [7]. The aspects of a catalytic reaction which are only dependent on local properties, such

* Corresponding author. Tel.: +1 520 626 5319; fax: +1 520 621 6048.
E-mail address: blowers@engr.arizona.edu (P. Blowers).

1381-1169/$ – see front matter © 2004 Elsevier B.V. All rights reserved.
doi:10.1016/j.molcata.2004.11.009

as activation of adsorbates and any bond breaking or forming that may take place, are in the realm of the cluster approach. On the other hand, properties that strongly depend on zeolite structures, like heats of adsorption and diffusion rates, are investigated by using embedding methods [8].

When studying heterogeneous zeolite reactions, an important issue is the choice of cluster model to describe the local environment around the zeolitic proton [9]. This Brønsted acidic site is generally modeled by one of the following cluster models:

$H–O–AlH_2–(OH)–H$ (1)

$H–O–Al(OH)_2–(OH)–H$ (2)

$H_3Si–O–AlH_2–(OH)–SiH_3$ (3)

$H_3Si–O–Al(OH)_2–(OH)–SiH_3$ (4)

The major differences among these cluster models lie in the number of tetrahedral (T) molecules (Al and Si) and the termination bonds (–H or –OH). Cluster models (1) and (2) contain only one tetrahedral molecule – aluminum, but no silicon – and are called T1 clusters. Cluster models (3) and (4) contain three tetrahedral structures – one aluminum and two silicons – and are called T3 clusters.

The silicon-containing cluster models have deprotonation energies close to those found for high-silica acidic zeolites, around 295.4 kcal/mol [10,11]. However, the computational requirements are greatly increased because of the two silicon atoms. Smaller silicon-free cluster models have higher deprotonation energies, which indicates that they are less strongly acidic and usually lead to higher activation energies. However, they are still useful when investigating reactions of large reactant molecules or the dependence of the reaction properties on cluster deprotonation energy. Cluster size effects on the reactions will be discussed later. The difference between cluster models (1) and (2) or (3) and (4) is in replacing the terminating hydrogens with hydroxyls connected to aluminum. Between the two silicon-containing cluster models, $H_3Si–O–Al(OH)_2–(OH)–SiH_3$ is closer to the real zeolite surroundings with only a slightly higher computational cost than $H_3Si–O–AlH_2–(OH)–SiH_3$. However, it has been shown that only small differences exist between the reaction energies of interest using these two models [12,13]. Additionally, convergence problems are sometimes encountered when seeking transition state structures using $H_3Si–O–Al(OH)_2–(OH)–SiH_3$ [11]. Therefore, the $H_3Si–O–AlH_2–(OH)–SiH_3$ cluster model is applied here to study ethane conversion reactions on zeolites, which are the main focus of this work.

Ab initio quantum chemistry has long been applied as a major tool for investigating the structure, stability, reaction kinetics and mechanisms of different molecular systems [14–23]. Blaszkowski et al. studied ethane conversion reactions using local density approximation (LDA) calculations, a low level density functional method [12]. Density functional theory and ab initio quantum chemical methods have been applied by other researchers to study catalytic reactions quantitatively [24–36]. However, for zeolite protonation systems, transition state energies could be underestimated by 30 kJ/mol. With the best calculations of the B3LYP method, the transition state energies may be underestimated by approximately 10 kJ/mol [10]. Kazansky et al. investigated the ethane cracking and dehydrogenation reactions using the small 3–21 basis set with a silicon-free T1 cluster [35]. The activation energies obtained are very high, bringing into question the validity of the results. With a T3 cluster model, Rigby et al. studied the ethane cracking reaction using MP2/6–31g*//HF/3–21g (energy calculation method//geometry optimization method). The results are still relatively high because of the small basis set applied in both geometry and energy calculation methods. More recently, Zygmunt et al. investigated the ethane cracking and dehydrogenation reactions using a T5 cluster. After higher-level theory corrections and long-range corrections, the activation energies obtained are 54.1 and 53.6 kcal/mol.

In this work, a silicon-containing T3 cluster is used to simulate the zeolite surface and ab initio methods are implemented to investigate the three ethane conversion reactions. The results are then compared with those from previous research. Furthermore, the influence of the zeolite cluster size and acidity on ethane conversion reaction activation energies is studied quantitatively. Also analytical formulas are provided in this work so activation energies can be obtained for different zeolite catalysts.

2. Computational methods

Electronic structure energy calculations traditionally consist of a single computation. However, in order to obtain accurate energetics, the calculation generally requires a very large basis set with a high level method and takes significant time to complete. Composite energy methods were invented in order to reach a high level of accuracy at a reduced computational cost. They are defined as a series of single point calculation steps whose results are combined to obtain the final electronic energy value. For instance, the complete basis set (CBS) methods have been developed recently [37–46]. These methods eliminate some of the empirical correlations that are included in the Gaussian-n series of methods while still giving very accurate predictions of heats of formation and enthalpies of reaction. Blowers and coworkers [47] proposed the CBS–RAD(MP2) compound model as a modification to the computationally expensive CBS–RAD model, which works especially well for free radicals with high spin contamination effects. The CBS–RAD(MP2) model replaces the time consuming QCISD(fc)/6–31g* geometry optimization and frequency calculation in the CBS–RAD method with the MP2(full)/6–31g* method and basis set while providing similar accuracy at a reduced computational cost. Hereafter, the CBS–RAD(MP2) method will be referred to as CBS.

In this work, the CBS compound model was used to investigate ethane conversion energetics on a zeolite cluster. All

Table 1
Calculated results using MP2/6–31g* and experimental data

	$H_3SiOAlH_2$ $(OH)SiH_3$[a]	Experimental data
H—Al distance (Å)	2.39	2.43 ± 0.03, 2.48 ± 0.04[b]
O—H vibrational frequency (cm^{-1})	3496	3600–3623[c]

[a] Calculated results using MP2/6–31g*.
[b] Refs. [50,51].
[c] Refs. [52–54].

of the ab initio calculations were performed with the GAUSSIAN98 [48] software package. Geometries were optimized at the HF/6–31g* and MP2(full)/6–31g* levels of calculation. Initial geometries for MP2(full)/6–31g* were obtained using HF/6–31g* optimization results. In some cases, a planar symmetry constraint of the carbon atoms of ethane with five cluster atoms (one Al, two O and two Si) was imposed in order to accelerate calculation. All products and reactants were verified with frequency calculations to be stable structures, and all transition states were found to be first-order saddle points with only one negative eigenvalue. Additionally, intrinsic reaction coordinate (IRC) calculations showed that each reaction linked the correct products with reactants. Zero point vibrational energies (ZPVE) were obtained from harmonic vibrational frequencies calculated at the MP2(full)/6–31g* level with a scaling factor of 0.9661 [49]. Frequencies were scaled with a factor of 0.9427 at the MP2(full)/6–31g* level.

In order to verify the computational method used in this work, zeolite cluster $H_3SiOAlH_2(OH)SiH_3$ geometry and frequency calculation results, together with the available experimental results, are compared and listed in Table 1. By NMR spectroscopy, the distances between acidic hydrogen and aluminum atom are measured to be 2.43 ± 0.03 Å and 2.48 ± 0.04 Å, respectively, by Freude et al. [50] and Kenaston et al. [51]. The calculated result using MP2/6–31g* is 2.39 Å, which is in excellent agreement with the experimental data. The vibrational frequency of the acidic H–O bond is 3496 cm^{-1} using the same method. Compared with experimental value between 3600 and 3623 cm^{-1} [52–54], the relative error is within 3%. This supports the geometry optimization level and basis set choice for representing the system well.

3. Results and discussion

3.1. Cracking reaction

$$CH_3CH_3 + H_3SiOAlH_2(OH)SiH_3 \rightarrow CH_4 + H_3Si(OCH_3)AlH_2OSiH_3$$

The cracking reaction consists of the C–C bond cleavage of ethane by the zeolite Brønsted acid proton. The proton attaches to one methyl group of the ethane reactant and forms methane and a surface oxide. The calculated transition state structure using the MP2/6–31g* method is shown in Fig. 1(a). The acidic proton has been transferred to the right carbon of ethane and a methane molecule is almost formed. The left methyl group of ethane becomes a planar structure and forms a carbenium ion together with the cluster structure. The zeolite cluster plays an important role in this reaction. The right oxygen of the cluster acts as a Brønsted acid, which donates a proton while the left oxygen acts as a Lewis base, which receives the methyl group.

The activation energies obtained from the MP2 geometry optimization method with CBS energy calculations is 71.39 kcal/mol. Unfortunately, direct comparison to experiment cannot be accomplished because there are no experimental activation energies available. The experimental activation energy for the propane and *n*-butane cracking reactions are 47 kcal/mol [55], and for the *iso*-butane cracking reaction is 57 kcal/mol [56]. Considering the fact that the protonation of ethane is certainly more difficult than that of propane and butane [35], the experimental activation energy for ethane cracking reaction should be larger.

The results obtained in this work are compared with the computational results from other researchers. As listed in Table 2, the activation energy obtained by Blaszkowski et al. [12] using the LDA density functional method is 69.78 kcal/mol, which is relatively lower because density functional theory has been known to often underestimate activation energies relative to experiment [14,57–61]. Another reason for the discrepancy in energies could be that the transition state structure is not fully optimized and four imaginary frequencies modes were present in their work. The result from Kazansky using HF/3–21g//HF/3–21g [35], 93.38 kcal/mol, is so high because of the small T1 cluster used and the fact that HF energy calculations tend to overestimate barrier heights [62–65]. Another result from Kazansky and Frash [32] upgraded the geometry optimization method to MP2(fc)/6–31++g**//HF/6–31g*. The activation energy obtained, 80.30 kcal/mol, is still high mostly because the MP2 method is known for over-predicting activation energies [62–65]. Rigby et al. [26] applied MP2/6–31g*//HF/3–21g calculations where the basis set is less than that of Kanzansky. But the application of a larger T3 cluster instead of T1 used by Kanzansky gives an activation energy of 78.00 kcal/mol. More recently, Zygmunt et al. [25] studied the reaction with a large T5 cluster. The result obtained by MP2(fc)/6–31g*//MP2(fc)/6–31g* is 73.70 kcal/mol. The authors then included higher level theory corrections by using MP2(fc)/6–311+g**//MP2(fc)/6–31g* and reduced the activation energy by 2.0 kcal/mol. The long-range correction obtained by the HF/6–31g* correction for 58T cluster model then reduces the activation energy by 14.50 kcal/mol. Including both corrections together with zero point energy correction and thermal corrections brings the activation energy to 54.10 kcal/mol.

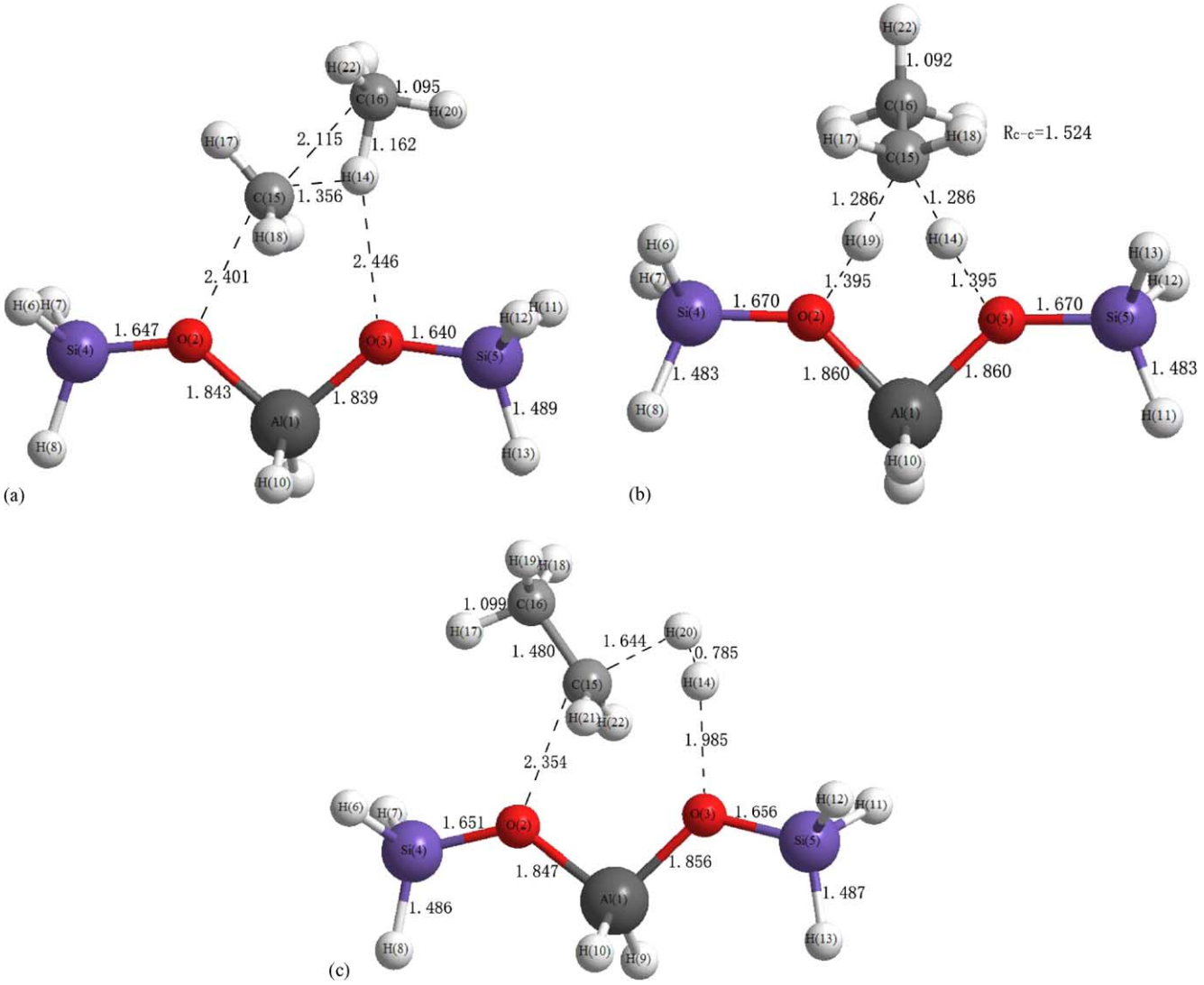

Fig. 1. Transition state structures for ethane reactions on zeolite cluster (a) cracking reaction, (b) hydrogen exchange reaction and (c) dehydrogenation reaction (units in Å).

Table 2
Activation energy calculation results for ethane conversion reactions on zeolites using the CBS method (units in kcal/mol)

	This work		Blaszkowski et al. [12]	Kazansky et al. [35,36]	Kazansky et al. [32]	Rigby et al. [26]	Zygmunt et al. [25]
Cluster model	T3	T3	T3	T1	T1	T3	T5
Geometry optimisation method	HF/6–31g*	MP2(full)/6–31g*	LDA/DZPV	HF/3–21g	HF/6–31g*	HF/3–21g	MP2(fc)/6–31g*
Energy calculation method	CBS-RAD(MP2)	CBS-RAD(MP2)	LDA/DZPV	HF/3–21g	MP2/6–31++g**	MP2/6–31g*	MP2(fc)/6–31g*
Cracking reaction	71.29	71.39	69.78	93.38	80.30	78.00	73.70/54.10[a]
Hydrogen exchange reaction	32.90	31.39	28.28	–	–	–	–
Dehydrogenation reaction	75.91	75.95	70.98	94.80	83.80	–	71.60/53.60[a,b]

[a] After corrections.
[b] Obtained by B3LYP/6–311g**//B3LYP/6-311g*.

3.2. Hydrogen exchange reaction

$$CH_3CH_3 + H_3SiOAlH_2(OH)SiH_3 \rightarrow CH_3CH_3 + H_3Si(OH)AlH_2OSiH_3$$

Fig. 1(b) shows the calculated transition state structure for the hydrogen exchange reaction of ethane using the MP2 method. It shows clearly the C_s symmetry obtained without any symmetry constraints applied for the optimization step. The carbon in the main plane of the zeolite structure, C(15), is pronated and becomes a penta-coordinated structure. The other carbon atom keeps its tetrahedral structure. The two hydrogen atoms, H(14) and H(19), stay in the middle of the carbon and oxygen atoms, indicating formation of one C–H bond and breaking of the other. The right oxygen of the cluster acts as a Brønsted acid, which donates a proton. The left oxygen acts as a Lewis base, which receives the hydrogen atom from ethane.

The activation energies obtained from the MP2 geometry optimization and the CBS energy is 31.39 kcal/mol. This barrier is the lowest among the three ethane conversion reactions, indicating it is the easiest reaction to take place. The activation energy obtained by Blaszkowski et al. [12] using LDA density functional theory, 28.28 kcal/mol, is somewhat lower than ours. There are no additional calculated results available for comparison.

3.3. Dehydrogenation reaction

$$CH_3CH_3 + H_3SiOAlH_2(OH)SiH_3 \rightarrow H_2 + H_3Si(OC_2H_5)AlH_2OSiH_3$$

The dehydrogenation reaction consists of cleavage of a C–H bond by the zeolite Brønsted acid proton. The transition state structure of the reaction is shown in Fig. 1(c). The carbon atom attached to the acidic proton becomes a planar structure and the other carbon keeps the tetrahedral structure. A six member ring, O(2)–Al(1)–O(3)–H(14)–H(20)–C(15), is formed. With the H(20)–C(15) and H(14)–O(3) distances greatly extended, a di-hydrogen molecule is almost formed whereas the C_2H_5 binds to the zeolite oxygen, O(2), which acts as a Lewis base.

The activation energies obtained from the MP2 geometry optimization with the CBS energy is 75.95 kcal/mol. This barrier is the highest among all three ethane conversion reactions, indicating it is the most difficult reaction to take place. Compared with other researchers work, this result is higher than the result obtained by Blaszkowski et al. [12] using LDA density functional theory, and much less than the results obtained by Kazansky et al. [32,35] using HF/3–21g//HF/3–21g and MP2/6–31++g**//HF/6–31g* calculations. Zygmunt studied this reaction with a large T5 cluster. The result obtained B3LYP/6–31g*//B3LYP/6–311g** is 71.60 kcal/mol. Similar to the study of the ethane cracking reaction, the authors then included the long-range correction obtained by the HF/6–31g* correction for the 58T cluster model and reduced the activation energy to 53.6 kcal/mol.

3.4. Geometry optimization method

In this work, both HF and MP2 optimization methods combined with the same basis set, 6–31G*, were used to obtain the geometries of the reactants and transition states. The energies were then obtained by using the composite CBS method. As shown in Table 2, there is little difference between the activation energies obtained using these two different geometry optimization methods, with the maximum difference within 1 kcal/mol. The Hartree–Fock method, the most economical method in the ab initio family, is described by other researchers to fail in describing the motion of individual electrons, especially for the computation of hydrogen bonds and protonation [9]. However, this was not encountered in this work. Therefore, we find that the calculated activation energies depend greatly on the level of energy calculation method and depend less on the level of geometry optimization method. Using high level calculations to obtain the activation energies through CBS energy calculation methods is crucial in this situation. Therefore, the geometry optimized using the HF method is adequate for activation barriers as long as the final energy is obtained using a high level method like CBS. Because of the low computational cost of the HF geometry optimization method, it is recommended for studying other zeolite catalytic reactions of large hydrocarbon species.

3.5. Cluster size effect

The choice of cluster to represent the zeolite surface plays a very important role in studying reaction properties. In this work, we investigated the effect of the cluster size for the ethane cracking reaction. The smallest cluster chosen is H–O–AlH_2–(OH)–H, a silicon-free T1 cluster. The deprotonation energy (E_{dep}) of a cluster is a good indication of its chemical properties, and is defined as the energy difference between the protonated (ZH) and unprotonated (Z^-) clusters [66]

$$E_{dep} = E(Z^-) - E(ZH)$$

The deprotonation energy of this small cluster, 318.26 kcal/mol, is much higher than the average zeolite value, 295.40 kcal/mol [10,11], which indicates a stronger bonding between the acidic hydrogen and its oxygen neighbor. Therefore, for small clusters, it takes more energy to break the H–O bond so the cracking reaction can take place, which means a higher activation barrier. The activation energies of the reaction and the corresponding deprotonation energies of the clusters are listed in Table 3 together with those obtained using the larger T3 cluster H_3Si–O–AlH_2–(OH)–SiH_3.

Since the clusters do not have exactly the same deprotonation energy as real zeolite catalysts, corrections can be made

Table 3
Calculated activation energy for the ethane cracking reaction with different cluster sizes and the average zeolite catalyst (units in kcal/mol)

	Deprotonation energy	Activation energy
$HOAlH_2(OH)H$	318.26	78.02
$H_3SiOAlH_2(OH)SiH_3$	298.02	71.39
Average zeolite[a]	295.40	70.52

[a] Refs. [10,11].

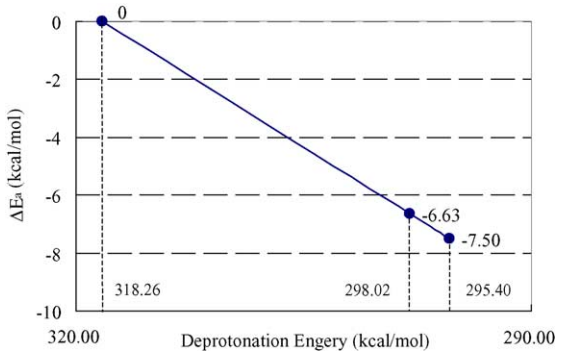

Fig. 2. Corrections to the calculated ethane cracking reaction activation energies for the cluster size effect.

in order to obtain accurate activation energies. Applying the Brønsted–Polanyi principle, the following relationship can be used [67]

$$\Delta E_a = c\Delta E_{dep}$$

As long as the reaction mechanism does not alter, the change in activation energy is linearly correlated to the change in deprotonation energy. Fig. 2 is a plot of the activation energy change against deprotonation energy of the clusters. A linear extrapolation is made to extend the curve to the average zeolite catalyst deprotonation energy point, 295.40 kcal/mol, and the activation energy obtained is 70.52 kcal/mol. The relationship can be described as

$$\Delta E_a = 0.3279E_{dep} - 104.37$$

Kazansky et al. studied the cluster size effect of the cracking reaction using the smaller $HOAl(OH)_2(OH)H$ and larger $H_3SiOAlH_2(OH)SiH_3$ clusters [11,30]. The relationship between ΔE_a and E_{dep} is correlated as: $\Delta E_a = 0.3213E_{dep} - 102$. The slope is almost identical between the work of Kanzansky and this work, even though the energy calculation methods are very different (MP2 for Kanzansky and CBS for this work). The difference of the constant term is caused by the deprotonation energy difference between the $HOAl(OH)_2(OH)H$ cluster used by Kanzansky and the $HOAlH_2(OH)H$ cluster used in this work. Therefore, the slope between the reaction activation energy and the cluster deprotonation energy is a constant that does not depend on the energy calculation method chosen, even while the deprotonation energy may depend on the method.

3.6. Acidity effects

The deprotonation energy is a theoretical measurement of zeolite acidity. It has been show by Kramer et al. [68,69] that the acidity effect of zeolite catalysts can be simulated by modifying the peripheral bonds of the cluster model. In real zeolite catalysts, the proton affinity varies over the range of 20–50 kcal/mol among different zeolite structures. This can be mimicked by assigning different bond lengths to the terminal Si–H bonds of the cluster with all other geometry parameters optimized. Fig. 3 shows the effect of Si–H distance on the zeolite cluster geometries. With increases of the Si–H bond length, the neighbor Si–O bond length decreases. The O–H bond length increases slightly from 0.978 to 0.982 Å as the Si–H bond length changes from 1.30 to 1.70 Å. This indicates that the O–H bond becomes weaker with the increasing distance of the Si–H bond. Therefore, the zeolite cluster becomes more acidic. The Al–O and O–Si distances on the far end of the changing Si–H bond vary almost negligibly because the atoms are too far away. Increasing the Si–H bond length on the left side of the cluster only has a slight effect on the O–H bond because the Si and H atoms are so far apart.

The changes of the zeolite acidity also affect the transition state structures and activation energies of the reactions. Fig. 4 shows the transition state structures of the ethane cracking reaction as the Si–H distance changes. With the Si–H bond length increase, the CH_3 product moves further from the cluster and the CH_4 product moves further from the cluster. Meanwhile, the CH_3 and CH_4 groups get closer to each other.

Table 4 shows the change in activation energies as the Si–H bond distances for ethane cracking, dehydrogenation and hydrogen exchange reactions are varied. With the Si–H distance increasing, the activation energies decreases for all three reactions because of the increased acidity of

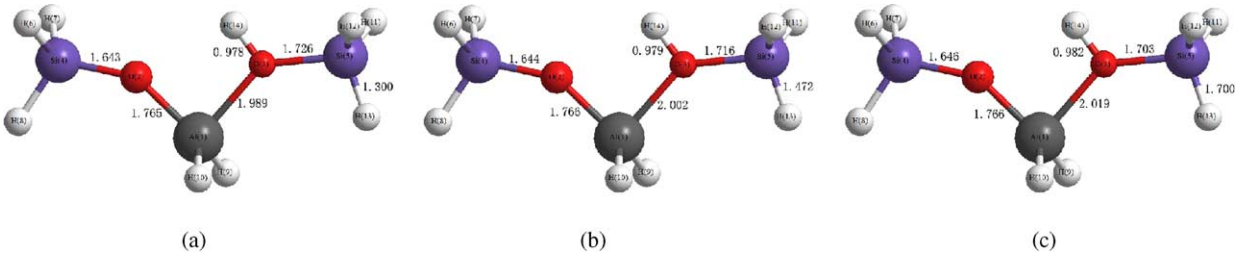

Fig. 3. $H_3Si{-}O{-}AlH_2{-}(OH){-}SiH_3$ cluster structures with changing terminate Si–H bond distances (units in Å): (a) R_{Si-H} = 1.3 Å (less acidic), (b) R_{Si-H} = 1.47 Å (equilibrium) and (c) R_{Si-H} = 1.7 Å (more acidic).

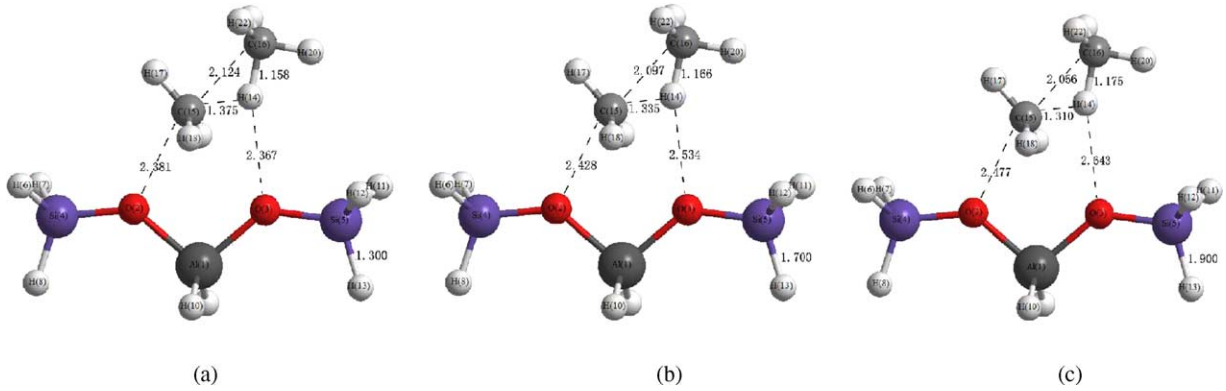

Fig. 4. Transition state structures of ethane cracking reaction with changing terminate Si—H bond distances (units in Å): (a) $R_{Si—H}$ = 1.3 Å (less acidic), (b) $R_{Si—H}$ = 1.7 Å (more acidic) and (c) $R_{Si—H}$ = 1.9 Å (most acidic).

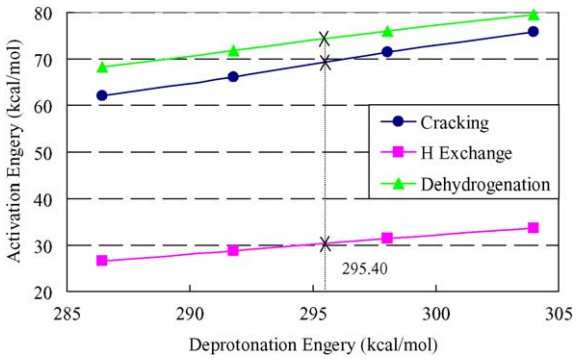

Fig. 5. Corrections to the calculated ethane conversion reactions activation energies for the acidity effect.

the zeolite cluster. The relationship of the activation barriers with cluster deprotonation energies is illustrated in Fig. 5. The linear dependence between these properties is seen, and the expressions are listed in Table 4. Applying the average zeolite catalyst deprotonation energy, 295.40 kcal/mol, the activation energies are then calculated and listed in Table 4. For the ethane cracking reaction, the activation barrier obtained is 69.08 kcal/mol using the expression $E_a = 0.7887E_{dep} - 163.90$. There is only a 1.50 kcal/mol difference with the results obtained from the cluster size effect correlation compared to the previous section, 70.52 kcal/mol. Because of the different types of zeolite catalysts used, the activation energies change slightly.

The acidity effect study has shown that there is a correlation between the deprotonation energy and activation energy for ethane conversion reactions. This is important because deprotonation energies are significantly easier to calculate than activation energies due to the difficulty in performing transition state optimizations for large complexes with many degrees of freedom. One correlation showed that the deprotonation energy can be varied by varying the cluster size, allowing one to now predict how ethane conversion reaction results may be extrapolated to larger cluster sizes. The second correlation showed how one could vary peripheral bonds on the cluster to change the deprotonation energy and influence the activation energy. Applying the expressions, activation energies can be obtained for different zeolite catalysts as long as the experimental deprotonation energy is first acquired.

4. Conclusions

In this work, ethane cracking, hydrogen exchange and dehydrogenation reactions catalyzed by a zeolite were studied using ab initio methods. The transition state structures were optimized using HF and MP2 methods, and the energies were obtained using a CBS composite energy method. The effects of zeolite cluster size and acidity on the activation barriers were investigated. Additionally, the choice of HF and MP2 geometry optimization methods and the effects on the barrier heights were also studied.

Table 4
Effects of Si—H distances on activation energies (units in kcal/mol)

	Activation energy (E_a)			Deprotonation energy (E_{dep})
	Cracking	Dehydrogenation	Hydrogen exchange	
$R_{Si—H}$ = 1.30 Å	75.74	79.52	33.64	303.97
$R_{Si—H}$ = 1.47 Å	71.39	75.95	31.39	298.02
$R_{Si—H}$ = 1.70 Å	66.12	71.71	28.70	291.76
$R_{Si—H}$ = 1.90 Å	62.03	68.16	26.63	286.44
Average zeolite[a]	69.08	74.04	30.23	295.4

Empirical correlation: $E_a = 0.7887E_{dep} - 163.90$ $E_a = 0.6509E_{dep} - 118.23$ $E_a = 0.403E_{dep} - 88.82$.
[a] Refs. [10,11].

The activation energies obtained for cracking, hydrogen exchange and dehydrogenation reactions are 71.39, 31.39 and 75.95 kcal/mol, respectively, using geometries optimized at the MP2 level. This indicates that the hydrogen exchange reaction has the lowest barrier and is the easiest reaction to happen, while the dehydrogenation reaction has the highest barrier and is the most difficult to happen.

The silicon-free T1 cluster was also used to study the ethane cracking reaction. The activation energy obtained, 78.02 kcal/mol, is much higher than that of the T3 cluster model because of its high deprotonation energy (or low acidity). The zeolite acidity effect was mimicked by changing the terminating Si–H bond lengths. Relationships between the activation energies and deprotonation energies were proposed so that accurate reaction barriers could be obtained when using zeolite catalysts with different acidities.

Acknowledgements

This work was funded by the State of Arizona through the office of the Vice President for Research at the University of Arizona. Supercomputer time was provided by the National Computational Science Alliance and used the NCSA HP/Convex Exemplar SPP-2000 at the University of Illinois at Urbana-Champaign. Part of the supercomputer time was provided by National Partnership for Advanced Computational Infrastructure and used the IBM pSeries 690 and pSeries 655 at Boston University.

References

[1] T. Maesen, B. Marcus, Introduction to Zeolite Science and Practice, 2nd ed., Studies in Surface Science and Catalysis, vol. 137, Elsevier 2001, p. 1.
[2] http://www.iza-structure.org/databases/.
[3] L.B. McCusker, C. Baerlocher, Introduction to Zeolite Science and Practice, 2nd ed., Studies in Surface Science and Catalysis, vol. 137, Elsevier 2001, p. 37.
[4] E.M. Flanigen, Introduction to Zeolite Science and Practice, 2nd ed., Studies in Surface Science and Catalysis, vol. 137, Elsevier 2001, p. 11.
[5] B.W. Wojciechowski, A. Corma, Catalytic Cracking: Catalysts, Chemistry and Kinetics, Dekker, New York, 1986.
[6] I.E. Maxwell, W.H.J. Stork, Introduction to Zeolite Science and Practice, Elsevier, Amsterdam, 1991.
[7] S.P. Bates, R.A. Van Santen, Adv. Catal. 42 (1998) 1.
[8] R.A. van Santen, J. Mol. Catal. A: Chem. 115 (1997) 405.
[9] R.A. van Santen, Catal. Today 38 (1997) 377.
[10] R.A. van Santen, B. van de Graaf, B. Smit, Introduction to Zeolite Science and Practice, 2nd ed., Studies in Surface Science and Catalysis, vol. 137, Elsevier 2001, p. 419.
[11] M.V. Frash, R.A. van Santen, Top. Catal. 9 (1999) 191.
[12] S.R. Blaszkowski, M.A.C. Nascimento, R.A. van Santen, J. Phys. Chem. 100 (1996) 3463.
[13] S.R. Blaszkowski, A.P.J. Jansen, M.A.C. Nascimento, R.A. van Santen, J. Phys. Chem. 98 (1994) 12938.
[14] B.J. Lynch, D.G. Truhlar, J. Phys. Chem. A 105 (2001) 2936.
[15] B.S. Jursic, J. Chem. Soc., Perkin. Trans. 2 (1997) 637.
[16] T.N. Truong, T.T.T. Truong, Chem. Phys. Lett. 314 (1999) 529.
[17] T.N. Truong, J. Chem. Phys. 113 (2000) 4957.
[18] P. Blowers, R. Masel, AIChE J. 46 (2000) 2041.
[19] M.W. Wong, L. Radom, J. Phys. Chem. A 102 (1998) 2237.
[20] M.W. Wong, L. Radom, J. Phys. Chem. 99 (1995) 8582.
[21] M.W. Wong, A. Pross, L. Radom, J. Am. Chem. Soc. 116 (1994) 6284.
[22] Y.T. Xiao, J.M. Longo, G.B. Hieshima, R.J. Hill, Ind. Eng. Chem. Res. 36 (1997) 4033.
[23] M. Saeys, M.F. Reyniers, G.B. Marin, J. Phys. Chem. A 107 (2003) 9147.
[24] P.J. Hay, A. Redondo, Y.J. Guo, Catal. Today 50 (1999) 517.
[25] S.A. Zygmunt, L.A. Curtiss, P. Zapol, L.E. Iton, J. Phys. Chem. B 104 (2000) 1944.
[26] A.M. Rigby, G.J. Kramer, R.A. van Santen, J. Catal. 170 (1997) 1.
[27] S.J. Collins, P.J. Omalley, J. Catal. 153 (1995) 94.
[28] M.V. Frash, V.B. Kazansky, A.M. Rigby, R.A. van Santen, J. Phys. Chem. B 102 (1998) 2232.
[29] J. Abbot, P.R. Dunstan, Ind. Eng. Chem. Res. 36 (1997) 76.
[30] V.B. Kazansky, M.V. Frash, R.A. van Santen, Appl. Catal. A: Gen. 146 (1996) 225.
[31] V.B. Kazansky, Catal. Today 51 (1999) 419.
[32] V.B. Kazansky, M.V. Frash, R.A. van Santen, Proceedings of the Eleventh International Congress on Catalysis – 40th Anniversary, Parts A and B (Studies in Surface Science and Catalysis), vol. 101, 1996, p. 1233.
[33] S.J. Collins, P.J. Omalley, Chem. Phys. Lett. 228 (1994) 246.
[34] P. Viruelamartin, C.M. Zicovichwilson, A. Corma, J. Phys. Chem. 97 (1993) 13713.
[35] V.B. Kazansky, I.N. Senchenya, M. Frash, R.A. Vansanten, Catal. Lett. 27 (1994) 345.
[36] V.B. Kazansky, M.V. Frash, R.A. Vansanten, Catal. Lett. 28 (1994) 211.
[37] G.A. Petersson, A. Bennett, T.G. Tensfeldt, M.A. Allaham, W.A. Shirley, J. Mantzaris, J. Chem. Phys. 89 (1988) 2193.
[38] J.A. Montgomery, M.J. Frisch, J.W. Ochterski, G.A. Petersson, J. Chem. Phys. 112 (2000) 6532.
[39] T. Morihovitis, C.H. Schiesser, M.A. Skidmore, J. Chem. Soc., Perkin. Trans. 2 (1999) 2041.
[40] J.A. Montgomery, M.J. Frisch, J.W. Ochterski, G.A. Petersson, J. Chem. Phys. 110 (1999) 2822.
[41] P.M. Mayer, C.J. Parkinson, D.M. Smith, L. Radom, J. Chem. Phys. 108 (1998) 9598.
[42] P.M. Mayer, C.J. Parkinson, D.M. Smith, L. Radom, J. Chem. Phys. 108 (1998) 604.
[43] J.W. Ochterski, G.A. Petersson, J.A. Montgomery, J. Chem. Phys. 104 (1996) 2598.
[44] J.A. Montgomery, J.W. Ochterski, G.A. Petersson, J. Chem. Phys. 101 (1994) 5900.
[45] G.A. Petersson, M.A. Allaham, J. Chem. Phys. 94 (1991) 6081.
[46] G.A. Petersson, T.G. Tensfeldt, J.A. Montgomery, J. Chem. Phys. 94 (1991) 6091.
[47] X. Zheng, P. Blowers, Fuel Processing Technology, submitted for publication.
[48] M.J. Frisch, G.W. Trucks, H.B. Schlegel, P.M.W. Gill, B.G. Johnson, M.A. Robb, J.R. Cheeseman, T. Keith, G.A. Petersson, J.A. Montegomery, K. Raghavachari, M.A. Al-Laham, V.G. Zakrzewski, J.V. Ortiz, J.B. Foresman, J. Cioslowski, B.B. Stefanov, A. Nanayakkara, M. Challacombe, C.Y. Peng, P.Y. Ayala, W. Chen, M.W. Wong, J.L. Andres, E.S. Replogle, R. Gomperts, R.L. Martin, D.J. Fox, J.S. Binkley, D.J. Defrees, J. Baker, J.P. Stewart, M. Head-Gordon, C. Gonzalez, J.A. Pople, Gaussian, Inc., Pittsburgh PA, 1995.
[49] A.P. Scott, L. Radom, J. Phys. Chem. 100 (1996) 16502.
[50] D. Freude, J. Klinowski, H. Hamdan, Chem. Phys. Lett. 149 (1988) 355.
[51] N.P. Kenaston, A.T. Bell, J.A. Reimer, J. Phys. Chem. 98 (1994) 894.

[52] M. Trombetta, T. Armaroli, A.G. Alejandre, J.R. Solis, G. Busca, Appl. Catal. A: Gen. 192 (2000) 125.
[53] L.M. Kustov, V.B. Kazansky, S. Beran, L. Kubelkova, P. Jiru, J. Phys. Chem. 91 (1987) 5247.
[54] M.A. Makarova, A.F. Ojo, K. Karim, M. Hunger, J. Dwyer, J. Phys. Chem. 98 (1994) 3619.
[55] T.F. Narbeshuber, H. Vinek, J.A. Lercher, J. Catal. 157 (1995) 388.
[56] C. Stefanadis, B.C. Gates, W.O. Haag, J. Mol. Catal. 67 (1991) 363.
[57] B.G. Johnson, P.M.W. Gill, J.A. Pople, J. Chem. Phys. 98 (1993) 5612.
[58] D. Porezag, M.R. Pederson, J. Chem. Phys. 102 (1995) 9345.
[59] M. Torrent, M. Duran, M. Sola, Theochem-J. Mol. Struc. 362 (1996) 163.
[60] E. Goldstein, B. Beno, K.N. Houk, J. Am. Chem. Soc. 118 (1996) 6036.
[61] J.L. Durant, Chem. Phys. Lett. 256 (1996) 595.
[62] B.G. Willis, K.F. Jensen, J. Phys. Chem. A 102 (1998) 2613.
[63] W.T. Lee, R.I. Masel, J. Phys. Chem. 100 (1996) 10945.
[64] W.T. Lee, R.I. Masel, J. Phys. Chem. 99 (1995) 9363.
[65] H. Yamataka, S. Nagase, T. Ando, T. Hanafusa, J. Am. Chem. Soc. 108 (1986) 601.
[66] H.V. Brand, L.A. Curtiss, L.E. Iton, J. Phys. Chem. 97 (1993) 12773.
[67] R.A. van Santen, J.W. Niemantsverdriet, Chemical Kinetics and Catalysis, Plenum Press, New York, 1995.
[68] G.J. Kramer, R.A. Vansanten, C.A. Emeis, A.K. Nowak, Nature 363 (1993) 529.
[69] E.M. Evleth, E. Kassab, L.R. Sierra, J. Phys. Chem. 98 (1994) 1421.